STRANGE QUARK PDF UNCERTAINTY AND ITS IMPLICATIONS FOR W/Z PRODUCTION AT THE LHC *

A. Kusina[a], T. Stavreva[b], S. Berge[c], F.I. Olness[a], I. Schienbein[b] K. Kovařík[d], T. Ježo[b], J.Y. Yu[a,b], K. Park[a]

[a]Southern Methodist University, Dallas, TX 75275, USA
[b]Laboratoire de Physique Subatomique et de Cosmologie
Université Joseph Fourier/CNRS-IN2P3/INPG
53 Avenue des Martyrs, 38026 Grenoble, France
[c]Institute for Physics (WA THEP), Johannes Gutenberg-Universität
55099 Mainz, Germany
[d]Institute for Theoretical Physics, Karlsruhe Institute of Technology
Karlsruhe, 76128, Germany

(Received January 15, 2013)

We investigate the impact of parton distribution functions (PDFs) uncertainties on W/Z production at the LHC, concentrating on the strange quark PDF. Additionally, we examine the extent to which precise measurements at the LHC can provide additional information on the proton flavor structure.

DOI:10.5506/APhysPolBSupp.6.219
PACS numbers: 12.38.–t, 13.60.Hb, 14.70.–e

1. Introduction

Parton distribution functions provide the essential link between the theoretically calculated partonic cross sections, and the experimentally measured physical cross sections involving hadrons and mesons. This link is crucial if we are to make incisive tests of the Standard Model (SM), and search for subtle deviations which might signal new physics.

We show that despite recent advances in the precision data and theoretical predictions [1–5], the relative uncertainty on the heavier flavors remains large. We will focus on the strange quark and show the impact of these uncertainties on the production of W/Z bosons at the LHC.

This work is based on Ref. [6], and further details can be found therein.

* Presented by A. Kusina at the Light Cone 2012 Conference, Kraków, Poland, July 8–13, 2012.

2. Extracting the strange quark PDF

In previous global analyses, the predominant information on the strange quark PDF $s(x)$ came from the difference of (large) inclusive cross sections for Neutral Current (NC) and Charged Current (CC) DIS. For example, at leading-order (LO) the difference between the NC and CC DIS F_2 structure function is proportional to the strange PDF. Because the strange distributions are small compared to the up and down PDFs, the $s(x)$ extracted from this measurement has large uncertainties. Lacking better information, it was commonly assumed the distribution was of the form

$$s(x) = \bar{s}(x) \sim \kappa \left[\bar{u}(x) + \bar{d}(x)\right] /2 \tag{1}$$

with $\kappa \sim 1/2$. This approach was used, for example, in the CTEQ6.1 PDFs [7], but it does not reflect the true uncertainty of $s(x)$, in fact, it reflects the uncertainty on the up and down sea which is well constrained by DIS measurements.

Beginning with CTEQ6.6 PDFs [8], the neutrino–nucleon dimuon data was included in the global fits to more directly constrain the strange quark[1]; thus, Eq. (1) was not used, and two additional fitting parameters were introduced to allow the strange quark to vary independently of the u and d sea.

In Fig. 1, we show the relative uncertainty bands for the CTEQ6.6 PDF error sets (outer/blue), and for CTEQ6.1 sets (inner/green). We observe that in the case of CTEQ6.6 the relative error on the strange quark is much larger than for the CTEQ6.1 set, particularly for $x < 0.01$, where the neutrino–nucleon dimuon data do not provide any constraints. We expect this is a more accurate representation of the true uncertainty.

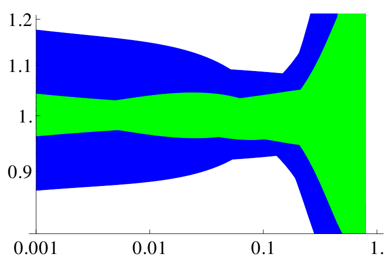

Fig. 1. Relative uncertainty of the s PDF as a function of x for $Q = 2$ GeV. The inner band is for CTEQ6.1, the outer for CTEQ6.6 PDF set.

This general behavior is also exhibited in other global PDF sets with errors [9–12]. Thus, there is general agreement that the strange quark PDF is poorly constrained, particularly in the small x region.

[1] For a detailed review of experimental constraints of strange PDF see Ref. [6].

3. Implications for Drell–Yan W/Z production at the LHC

The Drell–Yan production of $W^\pm$ and Z bosons at hadron colliders can provide precise measurements for electroweak observables, which can measure fundamental parameters of the SM. Furthermore, the W/Z-boson cross-section "benchmark" processes are intended to be used for detector calibration and luminosity monitoring; to perform these tasks, it is essential that we know the impact of the PDF uncertainties on these measurements. In the following, we will investigate the influence of the PDFs on the rapidity distributions of the Drell–Yan production process.

3.1. Strange contribution to W/Z production

Because the LHC has a different initial state and a higher CMS energy than the Tevatron, the relative contributions of the partonic subprocesses of the W/Z production change significantly. At the LHC, the contributions of the second generation quarks $\{s, c\}$ are greatly enhanced. In Fig. 2, we display how the different partonic cross sections contribute to W^+ production at LO. In Tevatron, the $u\bar{d}$ channel contributes 90% of the cross section, while contributions from strange quarks are comparably small $\sim$ 9%. At the LHC, subprocesses containing strange quarks are considerably more important. The $\bar{s}u$ channel contributes only 2%, while the $\bar{s}c$ channel yields 21%.

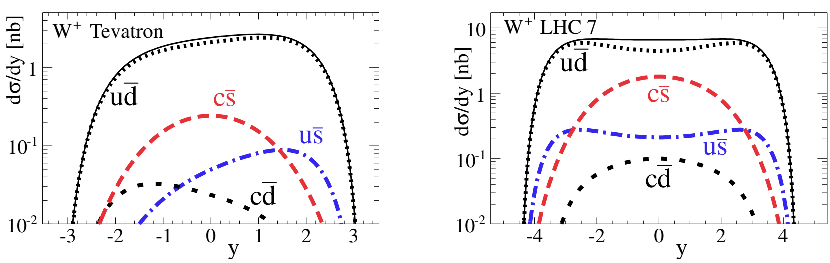

Fig. 2. Partonic contributions to $d\sigma/dy$ for W^+-boson production at LO at the Tevatron (left), and LHC with $\sqrt{S} = 7$ TeV (right).

We also note the LHC explores a much larger rapidity range. For channels containing strange quarks, $|y_{W/Z}|$ can be measured up to 4.5 at the LHC, compared to 2.5 at the Tevatron; therefore, smaller values of x of the strange quark distribution can be probed.

While the LO illustration of Fig. 2 provides a useful guide, in Fig. 3 we display the strange quark contribution to the differential cross section $d^2\sigma/dM/dy$ of on-shell $W^\pm/Z$ production computed at NNLO using [13]. The band (yellow) represents the strange-quark initiated contributions.

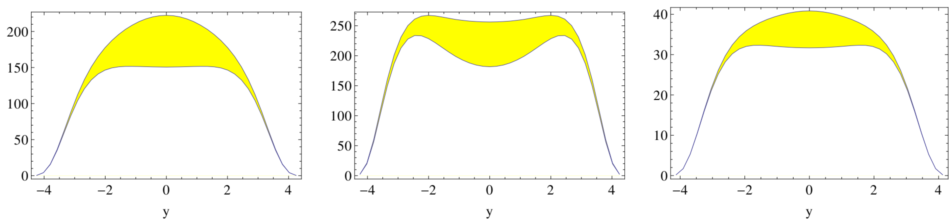

Fig. 3. $d^2\sigma/dM/dy$ in pb/GeV for $pp \to W^- + X$ (left), $pp \to W^+ + X$ (middle) and $pp \to Z, \gamma^* + X$ (right) production at the LHC for 7 TeV.

The figures impressively highlight the large contribution of the s and $\bar{s}$ quark subprocesses at the LHC. Consequently, it is essential to constrain the strange PDF if we are to make accurate predictions and to perform precision measurements. Figure 3 also shows the very different rapidity profiles of the strange quark and valence quark terms. This property is most evident for the case of W^+ production. Here, the dominant $u\bar{d}$ contribution has a twin-peak structure, while the $c\bar{s}$ distribution has a single-peak centered at $y = 0$. The total distribution is then a linear combination of the twin-peak and single-peak distributions, and these are weighted by the corresponding PDF.

Therefore, a detailed measurement of the rapidity distribution of the $W^\pm/Z$ bosons can yield information about the contributions of the s quark relative to the u, d quarks. As this is a relative measurement, it is reasonable to expect that this could be achieved with high precision once sufficient statistics are collected. Consequently, this is an ideal measurement where the LHC data could lead to stronger constraints on the PDFs.

Note, that ATLAS has already used W/Z production to infer constraints on the strange quark distribution, and they measured $r_s = 0.5(s + \bar{s})/\bar{d} = 1.00^{+0.25}_{-0.28}$ at $Q^2 = 1.9$ GeV^2 and $x = 0.023$ [14].

3.2. PDF uncertainty of the W/Z rapidity distributions

In Fig. 4 (left), we display the differential cross section $d^2\sigma/dM/dy$ for W^+ production at the LHC ($\sqrt{S} = 7$ TeV) using the 44 CTEQ6.6 error PDFs calculated at NNLO [13]. To better resolve these PDF uncertainties, in Fig. 4 (middle) we plot the ratio of the differential cross section $d^2\sigma/dM/dy$ compared to the central value. We observe that the uncertainty due to the PDFs as measured by this band is about $\pm 3\%$ for central boson rapidities.

For comparison, in Fig. 4 (right), we display the band (yellow) of CTEQ6.6 error PDFs of Fig. 4 (middle) together with the results using a selection of contemporary PDFs, all scaled by the central value of CTEQ6.6

set[2]. We observe that the choice of PDF sets can result in differences ranging to about $\pm 8\%$, which is well beyond the $\sim \pm 3\%$ displayed in Fig. 4 (middle).

While the band of error PDFs provides an efficient method to quantify the uncertainty, the range spanned by the different PDF sets illustrates that there are other important factors which should be considered.

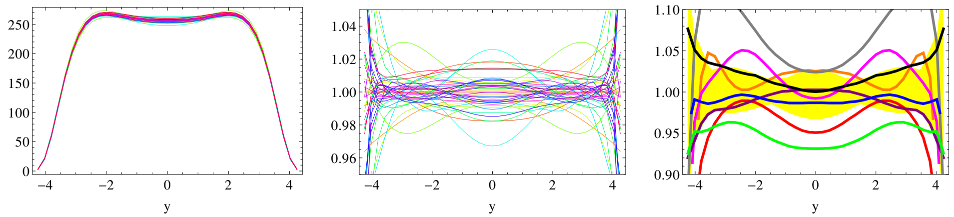

Fig. 4. Left: $d^2\sigma/dM/dy$ for $pp \to W^+ + X$ production at the LHC with CTEQ6.6 PDF set. Middle: Figure 4 (left) scaled by the central value. Right: Grey/yellow band representing $d^2\sigma/dM/dy$ for W^+ production with CTEQ6.6 set, compared with different PDF sets, all scaled by the central value of CTEQ6.6 set.

3.3. Correlations of the W/Z rapidity distributions

The leptonic decay modes of the W/Z bosons provide a powerful tool for precision measurements of electroweak parameters such as the W-boson mass. As the leptonic decay of the W boson contains a neutrino ($W \to \ell\nu$), the Z-boson production process ($Z \to \ell^+\ell^-$) is used to calibrate the leptonic W process. This method works to the extent the production processes of the W and Z bosons are correlated.

One possible measure to gauge the correlation of the PDF uncertainty is the ratio of the sum of the differential W^+ and W^- cross sections with respect to the differential Z-boson cross-section, normalized to the distribution of the central PDF set. We define

$$R = \left[\frac{d\sigma(W^+ + W^-)}{d\sigma(Z)}\right] \Big/ \left[\frac{d\sigma(W^+ + W^-)}{d\sigma(Z)}\right]_0 . \tag{2}$$

In Fig. 5, we plot R for the CTEQ6.5 and CTEQ6.6 PDF sets.

We observe that the uncertainty band in double ratios of Fig. 5 are much smaller than for single ratio of Fig. 4, which reflects the fact that W and Z processes are correlated. We also observe that the band for CTEQ6.5 (Fig. 5 (left)) is much smaller than for CTEQ6.6 (Fig. 5 (right)), meaning that correlation between W and Z processes is bigger when we use CTEQ6.5 PDFs.

[2] For details on the used PDFs see Ref. [6].

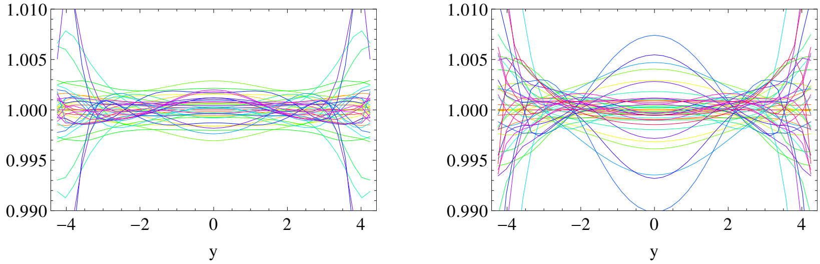

Fig. 5. Double ratio R as defined in Eq. (2) for the LHC with CTEQ6.5 (left) and CTEQ6.6 (right) calculated at NNLO.

The primary difference that is driving this result is the different strange PDF. For CTEQ6.5 the strange quark was defined by Eq. (1) while CTEQ6.6 introduced two extra fitting parameters which allowed the strange PDF to vary independently from the up and down sea. Thus, the uncertainty of the CTEQ6.6 distributions more accurately reflects the true uncertainty.

4. Conclusion

We have investigated the constraints of the strange PDFs and their impact on the W/Z-boson production at the LHC.

We observe that the strange quark is rather poorly constrained, particularly in the low x region which is sensitive to W/Z production at the LHC. Improved analyses from neutrino DIS measurements could help reduce this uncertainty. Conversely, precision measurements of W/Z production at the LHC may provide input to the global PDF analyses which could further constrain these distributions.

This work was partially supported by the U.S. Department of Energy under grant DE-FG02-04ER41299, and the Lightner Sams Foundation.

REFERENCES

[1] H. Abramowicz *et al.*, *Z. Phys.* **C25**, 29 (1984).

[2] J.P. Berge *et al.*, *Z. Phys.* **C35**, 443 (1987).

[3] A. Bazarko *et al.* [CCFR Collaboration], *Z. Phys.* **C65**, 189 (1995) [arXiv:hep-ex/9406007].

[4] S. Kretzer, H.L. Lai, F.I. Olness, W.K. Tung, *Phys. Rev.* **D69**, 114005 (2004) [arXiv:hep-ph/0307022].

[5] M. Tzanov *et al.* [NuTeV Collaboration], *Phys. Rev.* **D74**, 012008 (2006) [arXiv:hep-ex/0509010].

[6] A. Kusina *et al.*, *Phys. Rev.* **D85**, 094028 (2012) [arXiv:1203.1290 [hep-ph]].

[7] D. Stump *et al.*, *J. High Energy Phys.* **0310**, 046 (2003) [arXiv:hep-ph/0303013].

[8] P.M. Nadolsky *et al.*, *Phys. Rev.* **D78**, 013004 (2008) [arXiv:0802.0007 [hep-ph]].

[9] A. Martin, W. Stirling, R. Thorne, G. Watt, *Eur. Phys. J.* **C63**, 189 (2009) [arXiv:0901.0002 [hep-ph]].

[10] R.D. Ball *et al.*, *Nucl. Phys.* **B838**, 136 (2010) [arXiv:1002.4407 [hep-ph]].

[11] S. Alekhin, J. Blumlein, S. Klein, S. Moch, *Phys. Rev.* **D81**, 014032 (2010) [arXiv:0908.2766 [hep-ph]].

[12] P. Jimenez-Delgado, E. Reya, *Phys. Rev.* **D79**, 074023 (2009) [arXiv:0810.4274 [hep-ph]].

[13] C. Anastasiou, L.J. Dixon, K. Melnikov, F. Petriello, *Phys. Rev.* **D69**, 094008 (2004) [arXiv:hep-ph/0312266].

[14] G. Aad *et al.* [ATLAS Collaboration], *Phys. Rev. Lett.* **109**, 012001 (2012).